Estimating Finger Contact Location and Object Pose from Contact Measurements in 3-D Grasping

S. Haidacher and G. Hirzinger

German Aerospace Center - DLR
Institute for Robotics and Mechatronics
E-mail: `Steffen.Haidacher@dlr.de`

Abstract — *Autonomously grasping a predefined object is a topic of recent research in the field of service robotics. On the one hand, there are numerous approaches in the area of image processing concerned with recognition and localization of this object. On the other hand, a lot of work has been done in the development of planning, approaching and grasping of the object with a dextrous manipulator mounted on top of a robot arm. However, in-between locating and grasping, there are significant sources of uncertainty, e.g. estimation errors in image processing, errors in calibration of cameras and robot alone and with respect to each other, and positioning errors in the robot control. During the critical closing phase of grasping however, visual servoing and position correction is almost impossible to achieve due to obstruction of the object by the gripper. This paper presents an algorithm to locally estimate the position and orientation of the object to be grasped from contact information and a geometric description of the object. In this scenario, an object description is usually available to a sufficiently accurate extent from grasp planning.*
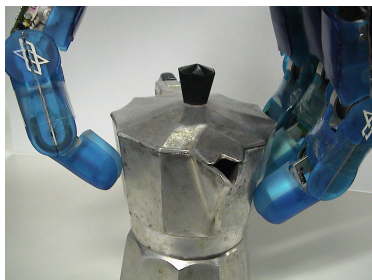
1   Introduction

Figure 1: DLR Hand II grasping an object

In recent years, in the field of robotic grippers and dextrous manipulators, a lot of developments have been brought forward. A general overview can be obtained from [2]. On the side of the gripper hardware, highly sophisticated devices are available with a large amount of sensory information [6, 12] (cf. fig 1). Based upon these, numerous algorithms have been presented to optimally plan [5], optimize and control [16] the grasp of a known or unknown object. Now,

in the field of service robotics, a system consisting of a mobile platform, an arm and an adequate gripper, is to work in a more complex environment. A typical task would be to detect an object of interest and localize it. Then a path for the approach of the arm has to be developed and the gripper positions for a stable grasp have to be computed. Finally the object can be grasped [15, 4]. However, the quality and robustness of the approach path and the grasp itself heavily relies on the accurateness of the localization of the object. The localization of the object however is in most cases done using global optical sensors. Although good for large scale path and grasp planing, these sensors wont render reliable values in the final phase of attaching the fingers to the object, because object or fingers may be obstructed from vision. To solve this problem, researchers propose object recognition and pose estimation using local sensors. Both steps are treated separately as *recognizing before locating* or in one step by *recognizing while locating* (cf. [9]). An early approach in the first group is given in [8], where contact features from a LSHGC description of objects are used to estimated pose of an object using tactile sensors. In [7] objects are examined using EPM models built up during tactile exploration. In the latter group, [9] uses a Kalman filter to determine the pose of a geometrically modeled object from an ultrasonic or infrared sensor. In [13] an unknown object is implicitly located and guided along a desired trajectory using tactile feedback. The approach taken in [11] observes an object in motion for pose estimation. [1] describes a system to combine visual and tactile sensing. These approaches all use either tactile information or visual sensing. Algorithms to exploit other sensory information rendering exteroceptive contact information, e.g. the position of contact and the direction of the surface normal of the finger and object surface in their common contact point are given in [3, 10].

This paper presents a blind man's approach to grasping. After blindly approaching an object, finger measurements are compared with a previously generated model. From this, by examining characteristics of the grasp and the object, hypotheses are generated for possible contact points of the fingers with the object.

The hypotheses are tested by finding a position and orientation of the grasped item relative to the gripper, that best complies with given measurements. Thus, this algorithm primarily implements the second step in *recognizing before locating*. Although theoretically working totally blindly, its main intention is to enhance the capabilities of other localization systems by giving more local information. This is helpful when these other systems are obstructed by scene objects as other items or a robotic arm or when a sufficient, absolute calibration between the location of the gripper and the localization system can not be obtained for example due to elasticity of the arm holding the gripper. In contrast to other algorithms for object localization known for example in the graphics and image processing community, the work presented here relies on the extremely sparse measurement of n fingers touching an object only once. On the side of the gripper, the measurements used to examine contact are either tactile readings from the finger tip or other information allowing determination of the contact point between the gripper and the grasped item. On the side of the object, no complete object description is required, since this approach is intended for local pose estimation. The model has to contain only those parts possibly encountered during grasping. In order to increase the performance of the algorithm, it is split into two parts, an offline refinement of the model and a online process setting up and testing contact hypotheses and estimating the object's orientation. This paper is structured as follows: The modeling is described in section 2. The refinement of the model and the determination of hypotheses is presented in sections 3.1 and 3.2 respectively. The test of hypotheses is described in section 4. Finally results of simulations and experiments are shown in section 5. In terms of notation, in this paper, superscripts $\diamond^{(x)}$ refer to the coordinate system $S^{(x)}$, subscripts $\diamond_o$ and $\diamond_c$ refer to object and contact quantities respectively, i and j refer to fingers, k and l to facets.

2 Modeling an Object

Most grippers available are capable of delivering contact information in one way or another. With a finger i contacting an object, detection of the point of contact $\tilde{\mathbf{x}}_{c,i}^{(w)}$ in the world reference frame $S^{(w)}$ and the direction of the normal vector $\tilde{\mathbf{n}}_{c,i}^{(w)}$ of the finger surface at this point can be achieved in one of two ways. Either tactile sensor information [14] can be used or appropriate algorithms [3, 10] may be applied to obtain this data from other sources of exteroceptive contact information as for example joint torques or finger velocities while moving over an object's surface. In graphics, this measurement is termed *oriented point*. It describes the tangential plane at the point of con-
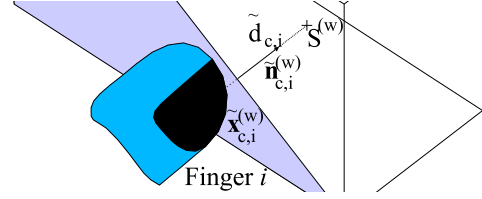

Figure 2: Measurement of facet plane at finger i

tact. With the contact information of each finger the object can be approximated locally around the contact points as seen from the fingers by a set $\mathcal{F}_c$ of tangent contact planes with distance $\tilde{d}_{c,i}^{(w)}$ from the origin $S^{(w)}$ as given in

$$
\begin{aligned}
0 &= \left(\tilde{\mathbf{n}}_{c,i}^{(w)}\right)^T \mathbf{r}^{(w)} + \tilde{d}_{c,i}^{(w)} \\
\tilde{d}_{c,i}^{(w)} &= -\left(\tilde{\mathbf{n}}_{c,i}^{(w)}\right)^T \tilde{\mathbf{x}}_{c,i}^{(w)}.
\end{aligned}
\tag{1}
$$

Figure 2 gives an overview over this description. Although there are many ways of modeling an object in 3 D (e.g. implicit description, B-splines), for the approach presented here a model that allows easy description of free form items and is only concerned about the surface and its normal direction is most suited to the measurement capabilities assumed for the gripper. Thus, the surface is represented by m triangular facets characterized by its vertices $\left(\mathbf{x}_{1,k}^{(o)}, \mathbf{x}_{2,k}^{(o)}, \mathbf{x}_{3,k}^{(o)}\right)$. This description can be obtained from usual CAD systems, scanning systems or easily be computed for simple objects. The accuracy of the description and hence the complexity of the task of detecting the effective finger contact positions on the object thus can easily be adapted by altering m. In the graphics society, there are numerous approaches available to simplify given models. It is conventional to arrange the vertices in a right hand sense with respect to the surface normal and to have the surface normal pointing out of the object. From the modeling, the vertices are given in an object related frame $S^{(o)}$. With this, a set $\mathcal{F}_o$ of object planes, each containing one triangular surface patch $k \in [1, m]$ can be formed by

$$
\begin{aligned}
0 &= \left(\mathbf{n}_{o,k}^{(o)}\right)^T \mathbf{r}^{(o)} + d_{o,k}^{(o)} \\
\mathbf{n}_{o,k}^{(o)} &= \left(\mathbf{x}_{2,k}^{(o)} - \mathbf{x}_{1,k}^{(o)}\right) \times \left(\mathbf{x}_{3,k}^{(o)} - \mathbf{x}_{1,k}^{(o)}\right) \\
d_{o,k}^{(o)} &= -\left(\mathbf{n}_{o,k}^{(o)}\right)^T \mathbf{x}_{o,k}^{(o)}.
\end{aligned}
\tag{2}
$$

Hereby the plane belonging to facet k is characterized by its surface normal $\mathbf{n}_{o,k}^{(o)}$ and the distance $d_{o,k}$ of the plane to the origin $S^{(o)}$. A schematic of the description is given in figure 3. It is to be noted that the normal vectors of two surfaces in contact are always anti-parallel. Thus a perfect measurement of a finger
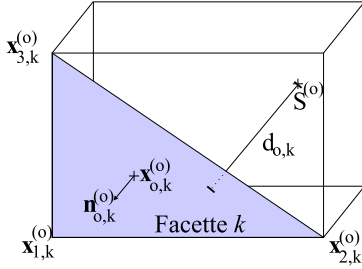
Figure 3: Description of a facet k

i contacting plane k would have a position value $\tilde{\mathbf{x}}_{c,i}^{(w)}$ in-between the vertices of k and its normal would be the negative of the facet. Thus, with the object in general and the contacts locally both being modeled as planes it is possible to search the object description $\mathcal{F}_o$ for an n-tuple of planes that best match the given measured set $\mathcal{F}_c$ of planes.

3 Examination of an Object

With n fingers grasping an object, there are m^n n-tuples of facets from $\mathcal{F}_o$. In order to perform a complete search on all tuples of planes from $\mathcal{F}_o$, the complexity of the algorithm would thus be in the order $O(m^n)$ of the number m of facets to the power of the number of fingers n. For usual objects with a sufficiently accurate model description and thus a sufficiently large number of facets m, this is neither feasible nor necessary. When grasping an object, conditions between individual fingers are set. Between two fingers the distance $\tilde{\Delta}_{ij} = \| \tilde{\mathbf{x}}_{c,j}^{(w)} - \tilde{\mathbf{x}}_{c,i}^{(w)} \|$ between the contact points of two fingers i and j as well as the angle $\alpha_{ij} = \arccos(\tilde{\mathbf{n}}_{c,i}^{(w)} \cdot \tilde{\mathbf{n}}_{c,j}^{(w)})$ between the respective surface normals can be obtained. They are relative, scalar measures between two facets and thus independent of coordinate systems, here the measurement system $S^{(w)}$ and the model system $S^{(o)}$. This restricts the number of admissible tuples from the whole set $\mathcal{F}_o$ of planes to only those that match the *grasp conditions* between the two fingers. On the other hand, for a given pairing of modeled facets k and l a range of possible distances $[\Delta_{min,kl}, \Delta_{max,kl}]$ and the angle α_{kl} between their surface normals can be given. These two values are characteristic for a given object. They can be computed offline when modeling an object and then held in a refined object description. Although also characteristic values of groupings of three or more finger can be used to characterize a grasp this increases the number of possible groupings as a power of m. Thus, the object description would be refined this way, allowing to sort out more facets that do not comply with these extended *grasp conditions*. However the model size would increase drastically. Hence the search in this larger object model would be prohibitively more time consuming. By using the proposed grasp conditions,

the number of facets tuples to further be examined can be reduced to a reasonable number. This offline process is described in section 3.1. The earlier proposed selection of facets after receiving measurements from the hand during an online detection phase is described in section 3.2. It is only this step, that is to be performed in real time. This method is comparable to a human, studying an object for example a cup, when first being confronted with it and on a later re-encounter using this information to easily pick it up at good positions, a problem of grasp planing [5], and verifying for this position, for example a flat spot on the surface or a handle, during grasp, as presented here.
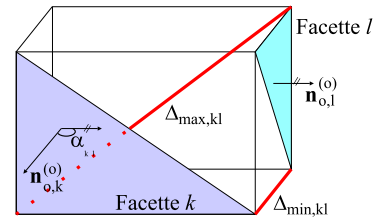
3.1 Modeling Phase

Figure 4: Characteristics of a facet pairing

This section is devoted to present the construction of a refined object description in order to accelerate the choice of admissible facet tuples. In order to study the geometrical dependencies of the facets in a given object model, the facets are numbered and a list of possible facet pairings $\mathcal{P}_2$ is formed. It is to be noted, that fingers may contact two on the same facet and also the ordering of fingers and respective facets is of importance. Thus, this list has dimension m^2. Its elements contain the numbers k and l of the respective facets, the maximum and the minimum Euclidean distance $\Delta_{min,kl}$ and $\Delta_{max,kl}$ between them and the angle α_{kl} between their surface normals $\mathbf{n}_{o,k}$ and $\mathbf{n}_{o,l}$. In order to compute the relative distances, it is sufficient to compare the $3^2 = 9$ possible distances between the vertices of the facets: Facets are part of planes that either are parallel or intersect. In the first case, all points in the facet have the same distance $\Delta_{min,kl} = \Delta_{max,kl}$, in the latter case the two vertices closest to the intersection line have minimum $\Delta_{min,kl}$ and those furthest of the line have maximum $\Delta_{max,kl}$ distance. These characteristic values are depicted in figure 4. For a faster and more robust selection of admissible facets in the online phase facet pairings are not treated individually but the characterized pairings from $\mathcal{P}_2$ are sorted into a three dimensional hash table $\mathcal{K}_3$. Each dimension represents one condition of the *contact constraints*. The $p_\diamond$ bins of the hash table are equidistantly spread over each axis and have width $q_\diamond$ with $\diamond \in \{\Delta_{min}, \Delta_{max}, \alpha\}$ and

$$Max_\diamond = \max_{kl} (\diamond_{kl})$$

$$Min_\diamond = \min_{kl}(\diamond_{kl})$$

$$q_\diamond = \frac{Max_\diamond - Min_\diamond}{p_\diamond}. \qquad (3)$$
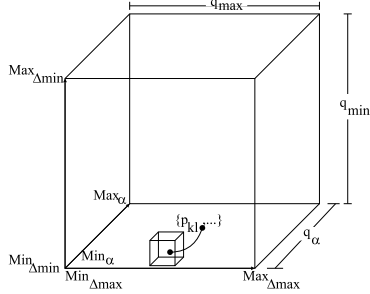
The hash table is depicted in figure 5. The hash func-

Figure 5: 3D Container $\mathcal{K}_3$ for sorted pairings

tions, used to access each coordinate of $\mathcal{K}_3$ are

$$t_1(\Delta_{max,kl}) = \text{floor}(\frac{\Delta_{max,kl} - Min_{\Delta max}}{q_{\Delta max}})$$

$$t_2(\Delta_{min,kl}) = \text{floor}(\frac{\Delta_{min,kl} - Min_{\Delta min}}{q_{\Delta min}})$$

$$t_3(\alpha_{kl}) = \text{floor}(\frac{\alpha_{kl} - Min_\alpha}{q_\alpha})$$

$$\text{with} \qquad t_1, t_2, t_3 \in I\!N. \qquad (4)$$

Thus, a pairing of facets k/l is inserted to bin $\mathcal{K}_3[t_1(\Delta_{max,kl}), t_2(\Delta_{min,kl}), t_3(\alpha_{kl})]$. With the facets sorted this way, a fast access during online computation is guaranteed. The choice of number of classes $p_\diamond$ and hence class width $q_\diamond$ determines the number of facets to be searched during an online phase.

3.2 Detection Phase

With measurements from n fingers available, admissible combinations of n respective facets have to be extracted from the container $\mathcal{K}_3$. With $\binom{n}{2}$ possible finger pairings also $\binom{n}{2}$ relative distances $\tilde{\Delta}_{ij}$ between the contact points $\tilde{\mathbf{x}}_{c,i}^{(w)}$ and angles $\tilde{\alpha}_i j$ between the surface normals $\tilde{\mathbf{n}}_{c,i}^{(w)}$ of fingers i and j (cf. figure 6) can be determined as *grasp conditions*. A list $\mathcal{S}_{ij}$ of
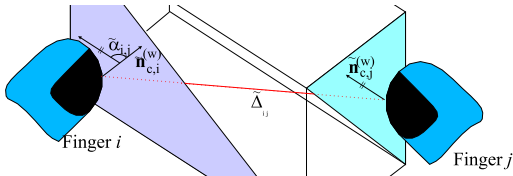

Figure 6: Characteristics of contact pair at fingers i,j

admissible facet pairs for each finger pairing i/j can be obtained from $\mathcal{K}_3$. Hereby the union of all facets whose maximum distance is at least $\tilde{\Delta}_{ij}$ and whose minimum distance is at most $\tilde{\Delta}_{ij}$ can be obtained according to

$$\mathcal{S}_{ij} = \cap_{a,b,c} \mathcal{K}_3[a,b,c]$$

$$a \in [t_1(\tilde{\Delta}_{ij} - \sigma_\Delta), p_{\Delta max}]$$

$$b \in [0, t_2(\tilde{\Delta}_{ij} + \sigma_\Delta)] \qquad (5)$$

$$c \in [t_3(\tilde{\alpha}_{ij} - \sigma_\alpha), t_3(\tilde{\alpha}_{ij} + \sigma_\alpha)].$$

Measurement noise and approximation errors when triangulating are accounted for by σ_Δ and σ_α. For a faster access these lists are best sorted and indexed. From these sorted lists of facet pairs, tuples of n facets
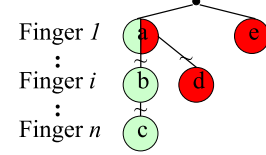

Figure 7: Search tree $\mathcal{T}$ for valid tuples

have to be formed. For this, a tree $\mathcal{T}$ is built with each level representing one finger and each node on a level representing admissible facets for the respective finger (cf. figure 7). The branches in the tree represent possible connections between facets for each finger and hence the admissible facet tuples. The tree can be build by first inserting list $\mathcal{S}_{12}$ in the tree. Then, parsing all nodes on the second level of $\mathcal{T}$, with finger two being on γ_2 and finger one being on the respective parent node γ_1, facet pairs of lists $\mathcal{S}_{13}$ and $\mathcal{S}_{23}$ are compared for entries with matching γ_3 in the third finger. On success a new node γ_3 is added on level three. Similarly lists $\mathcal{S}_{14}$, $\mathcal{S}_{24}$ and $\mathcal{S}_{34}$ are compared with finger three now on facet γ_3. This is repeated for all n fingers. After having constructed the tree, all paths ending at level n present appropriate hypotheses $\mathbf{h} = \gamma_1, ..., \gamma_n$ for contact positions of the respective fingers. In figure 7, a valid hypothesis is shaded bright (green) and ends at facet c, invalid hypotheses are shaded dark (red) and end at d and e.

4 Detection of Object Pose

Usually, *grasp constraints* do not limit the number of admissible facets to exactly one. Thus, multiple given hypotheses of finger contact locations have to be compared. This can be done by matching the facets of the hypotheses to the measurements, and thus determining the transform $\mathbf{T}_{(w)}^{(o)}(\theta, \mathbf{t}) = \left[\mathbf{R}_{(w)}^{(o)}(\theta)\mathbf{t}_{(w)}^{(o)}\right]$ between $S^{(o)}$ and $S^{(w)}$ and hence localizing the object. As admissible facets have only be constrained by pairs, not by measures for all n fingers, there will be hypotheses that allow better fit than others. The quality of a hypothesis can thus be determined. With the rotation angle being θ and the displacement being $\mathbf{t}$, the measured plane description of (1) can be mapped from $S^{(w)}$ to $S^{(o)}$ using

$$\mathbf{r}^{(w)} = \mathbf{R}_{(w)}^{(o)}(\theta)\mathbf{r}^{(o)} + \mathbf{t}_{(w)}^{(o)}$$

$$0 = \left(\mathbf{R}_{(w)}^{(o)}(\theta)^T\tilde{\mathbf{n}}_{c,i}^{(w)}\right)^T \mathbf{r}^{(o)} +$$

$$\left(\left(\tilde{\mathbf{n}}_{c,i}^{(w)} \right)^T \cdot \mathbf{t}_{(w)}^{(o)} + \tilde{d}_{c,i}^{(w)} \right). \qquad (6)$$

With this, an error function $\mathcal{L}$ can be developed which compares $\tilde{\mathbf{n}}_{c,i}^{(o)}$ and $\tilde{d}_{c,i}^{(o)}$ of the measured contact plane to $\mathbf{n}_{o,k}^{(o)}$ and $d_{o,k}^{(o)}$ of the respective object facet:

$$\mathcal{L}(\theta, \mathbf{t}) = \sum_{i=1}^{n} \left\{ \| \mathbf{R}_{(w)}^{(o)}(\theta)^T \tilde{\mathbf{n}}_{c,i}^{(w)} - \left(-\mathbf{n}_{o,k}^{(o)} \right) \|^2 + \left(\tilde{\mathbf{n}}_{c,i}^{(w)T} \cdot \mathbf{t}_{(w)}^{(o)} + \tilde{d}_{c,i}^{(w)} - \left(-\mathbf{n}_{o,k}^{(o)} \right) \right)^2 \right\}.(7)$$

The negative sign in front of model values originates in the opposing directions of the normal vectors on the object and the contacting finger tip. This function $\mathcal{L}$, computes the secant in the unit circle between the two normal vectors and the difference between the distances to the origin along the respective surface normal. A lateral displacement within the tangent plane cannot be measured and is hence not penalized. Minimizing $\mathcal{L}_{min,\mathbf{h}} = \min_{\theta,\mathbf{t}} \mathcal{L}(\theta, \mathbf{t})$ renders an estimate of the position $\mathbf{t}_{opt}$ and orientation θ_{opt} of the object with respect to $S^{(w)}$. Thus by testing for all $\mathbf{h}$ it is possible to choose the best fitting tuple of facets provided the measurements are accurate. Any previous measurement from vision or similar is taken into account as starting value. The optimization can be done using a standard Levenberg-Marquard algorithm.

5   Simulations and Experiments

The feasibility and computational behavior of the algorithms presented here have been tested in simulations and experiments. First, a model has to be obtained from an object to be grasped. Then, this object is examined in computer simulations. In order to be able to grasp real world objects, a method has to be found to model these objects without having to rely on CAD data from specially designed objects or simple geometries. At our institute, a rotating laser scanner has been developed, that renders information on the distance of objects in its scan [17]. Using joint readings of a hand guidable arm of Faro Inc. the position of the scanner and the obtained distance information can be combined to form a three-dimensional cloud of points representing the surface of the object. This cloud is processed by an algorithm, developed at our institute to render image files in *Open Inventor* format. Usually, this data contains a fairly high amount of triangular facets. For a examination of an object based on tactile sensor data, the resolution is far to fine. Thus the program *Jade2* by Scopigno and Cignoni is used to reduce the amount of triangles. On the other hand, since only local data is needed for determining object pose, the number of triangles can be reduced further if not all surface parts are feasible for

contact. The examples have been designed for DLR Hand II, thus the number n of fingers is 4. The number m of facets varies in the examples. The following computer simulations have been performed on a Sun Ultra II machine using only one processor with 750 MHz. First, a synthetic model of a banana is examined as depicted in figure 8. It has been reduced from 512 facets to $m = 53$ facets (cf. fig. 9) . One can clearly see the increased coarseness. However the object is still pretty well represented. The refinement
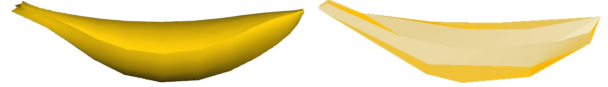

Figure 8: Banana   Figure 9: Red. Banana

of the model and the computation of characteristics $\mathcal{P}_2$ took $21ms$. The sorting into the database $\mathcal{K}_3$ required $19ms$. Thus the total preparation time was $40ms$. Now a random generator selects four facets for all four fingers. The object is rotated around its roll axis for 5.7^o and shifted in x- y- and z-direction for $10mm$. The algorithm is provided with the center of gravity of the selected facets of the rotated object. It returned the appropriate pose and orientation of the banana according to the given measurement for a wide range of initial values. The computational load for selection of facet sets S_{ij} was $24ms$. The computational load for building up the tree $\mathcal{T}$ and testing all possible hypotheses was in average over 25 runs with different facets $92ms$, with a minimum of $16ms$ and a maximum of $324ms$. This sums to an average time of $116ms$ during the online phase. Since localization does not have to be performed within a closed control loop, this time is feasible. Obviously, the computational load however varies heavily with the tuple of facets being randomly selected as measurement. This is a result of the possibility to sort out a different number of facets during the construction of the lists S_{ij}. Thus the load for computing the tree and hence for testing the hypotheses varies. As a second example, a real world espresso

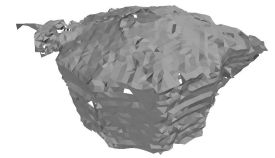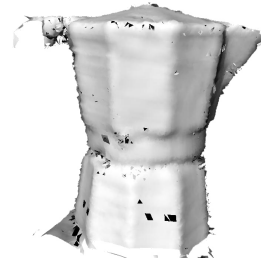Figure 10: Espr. machine   Figure 11: Red. Model

coffe maker is to be grasped with DLR Hand II (cf.fig. 1).The object has been scanned and modeled in its original version by 83846 facets (s. figure 10). The object has been re-sampled and regions of little interest have been cut off. The number of facets could thus be reduced to 6767 (s. figure 11). These facets have
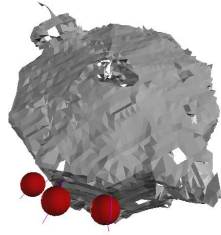
Figure 12: Estimated Grasp

been provided to the algorithm with some restrictions for each finger in order to reduce the search time. The algorithm was able to locate the object regardeless of errors in measurement and model to a satisfying extent (cf. fig 12)

6 Conclusion

In order to allow robotic grippers to grasp real world objects with uncertainty in their location, we here presented an approach to determine the most likely set of contact positions of fingers on the object together with an estimate of the objects pose as seen from the fingers. The object has been modeled by a triangulated surface. This way general surfaces can be treated. An approach has been presented to first refine the object description offline by characteristic relations between its facets and store those values in an object description. This allows faster access during an online phase. After receiving tactile measurements from the robotic hand, this database is searched for possible matching facet combinations. These facet combinations are used to determine the position of the object relative to the hand. The validity and computational behavior has been examined in simulations and experiments. In ongoing research this algorithm is enhanced to increase robustness and computational performance.

References

[1] P. K. Allen, A. T. Miller, P. Y. Oh, and B. S. Leibowitz. Using tactile and visual sensing with a robotic hand. In *Proceedings of the IEEE International Conference on Robotics and Automation, April 1997, Albuquerque, New Mexico*, 1997.

[2] A. Bicchi and V. Kumar. Robotic grasping and manipulation. In S. Nicosia, B. Siciliano, A. Bicchi, and P. V. (eds.), editors, *Ramsete: Articulated and mobile robots for services and Technology*, volume 270, chapter 4, pages 55–74. Springer-Verlag, Berlin Heidelberg, Germany, 2001. .

[3] A. Bicchi, J. K. Salisbury, and D. L. Brock. Contact sensing from force measurements. *International Journal of Robotics Research*, 12(3), 1993.

[4] C. Borst, M. Fischer, S. Haidacher, H. Liu, and G. Hirzinger. Dlr hand ii: Experiments and experiences with an anthropomorphic hand. In *submitted to ICRA 2003*, 2003.

[5] C. Borst, M. Fischer, and G. Hirzinger. A fast and robust grasp planner for arbitrary 3d objects. In *Proc. IEEE Conf. on Robotics and Automation*, pages 1890–1896, Detroit, Michigan, May 1999. .

[6] J. Butterfass, M. Grebenstein, H. Liu, and G. Hirzinger. DLR-Hand II: Next Generation of Dextrous Robot Hand. In *Proc. IEEE Conf. on Robotics and Automation*, pages 109 – 114, Seoul, Korea, May 2001. .

[7] S. Caselli, C. Magnanini, F. Zanichelli, and E. Caraffi. Efficient exploration and recognition of convex objects based on haptic perception. In *Proceedings of the IEEE International Conference on Robotics and Automation, April 1996, Minneapolis, Minnesota*, 1996.

[8] R. S. Fearing. Tactile sensing for shape interpretation. In S. Venkataraman and T. Iberall, editors, *Dextrous Robot Manipulation*, chapter 10. Springer-Verlag, 1990.

[9] J. D. Geeter, H. V. Brussel, J. D. Schutter, and M. Decrton. Recognizing and locating objects with local sensors. In *Proceedings of the IEEE International Conference on Robotics and Automation, April 1996, Minneapolis, Minnesota*, 1996.

[10] S. Haidacher and G. Hirzinger. Contact point identification in multi-fingered grasps using kinematic constraints. In *Proceedings of the IEEE International Conference on Robotics and Automation May 2002, Washington,D.C. ,USA*, 2002.

[11] Y. B. Jia and M. Erdmann. Pose and motion from contact. *International Journal of Robotics Research*, 18(5):466 – 490, May 1999.

[12] C. S. Lovchik and M. A. Diftler. The robonaut hand: A dextrous robot hand for space. In *Proc. IEEE Conf. on Robotics and Automation*, pages 907 – 912, Detroit, Michigan, USA, May 1999.

[13] H. Maekawa, K. Tanie, and K. Komoriya. Tactile sensor based manipulation of an unknown object by a multifingered hand with rolling contact. In *Proceedings of the IEEE International Conference on Robotics and Automation, May 1995, Nagoya, Japan*, 1995.

[14] A. M. Okamura, M. L. Turner, and M. R. Cutkosky. Haptic exploration of objects with rolling and sliding. In *Proceedings of the IEEE International Conference on Robotics and Automation, April 1997, Albuquerque, New Mexico*, 1997.

[15] L. Petersson, P. Jensfelt, D. Tell, M. Strandberg, D. Kragic, and H. I. Christensen. System Integration for Real-World Manipulation Tasks. In *Proc. of IEEE Intl. Conference on Robotics and Automation*, pages 2500 – 2505, Washington DC, USA, May 2002.

[16] T. Schlegl, M. Buss, T. Omata, and G. Schmidt. Fast dextrous regrasping with optimal contact forces and contact sensor-based impedance control. In *Proceedings of the IEEE International Conference on Robotics and Automation May 2001, Seoul ,Korea*, 2001.

[17] M. Suppa. Miniaturisierter laserscanner fuer robotikanwendungen. *Mechatronik-News, Informationen des Bayrischen Kompetenznetzwerkes fuer Mechatronik*, (1), 2002.